FULL LENGTH PAPER

CFD DRIVEN AERO-PROPULSIVE DESIGN OF A DUCTED RAMJET MISSILE

Anand Bhandarkar, M.S.R Chandra Murty, P. Manna, Debasis Chakraborty
Directorate of Computational Dynamics
Defence Research and Development Laboratory (DRDL)
Kanchanbagh Post, Hyderabad-500 058, India
Email : debasis_cfd@drdl.drdo.in; debasisc.cfd@gmail.com

Abstract

Detailed Computational Fluid Dynamics (CFD) simulations are carried out for a ducted ramjet missile. Combined internal and external flow fields are numerically simulated by solving 3D RANS equations along with Menter's SST turbulence model. Aero-propulsive configuration is evolved progressively by improving radome shape, intake ramps, intake bleed system, diverter height etc. Numerical simulations have revealed that ogive radome has less drag compared to power law shaped radome and provide better flow characteristics at the intake entry leading to superior intake performance. Appropriate boundary layer diverter height and bleed system in the intake improve the intake performance. Aero-propulsive performance of the complete vehicle is estimated for different Mach numbers and angles of attack. It is demonstrated that improved performance of the ducted ramjet missile can be obtained through use of high fidelity numerical method.

Keywords*: Air Breathing Missile, Combined External Internal Flow CFD, Solid Fuel Ramjet, Air Intake*

Introduction

Extended range, sustained speed, better maneuverability and superior end game has made the ramjet system an ideal propulsion choice for supersonic tactical missile [1-4]. Recently, variable flow ducted rockets (hybridisation between ramjet and rocket) are extensively studied by many researchers [5-9] due to their long flight range as well as high speed in terminal phase due to its thrust controllability. The schematic of variable flow ducted rocket is shown in Fig.1. These engines uses an integrated solid/liquid rocket motor to accelerate the missile to a Mach number suitable for ramjet operation. In the ramjet phase, the engine takes the exhaust from a liquid/solid fuel gas generator, mixes it with air, and burns it to produce thrust.

During air-breathing cruise phase, the vehicle thrust and drag need to be same. Hence, thrust requirement increases with increased drag. Higher thrust demand requires a higher fuel to air ratio, while the specific impulse of ram propulsion systems decreases with the reduced air. High thrust demand asks for optimum mixing of complete air flow with the propellant in the combustor. A low drag configuration with high amount of excess air is best suited for a staged air injection. Hence, the accurate estimation of drag and thrust and the optimization of these parameters become very important for the success of ramjet propulsion based aerospace vehicles.

Radome shapes and positioning of the air intakes influences the missile drag very significantly. Different Radom shapes (ogive/power law) have been adopted in different missile systems to reduce fore-body drag and flow distortions in the intake entry. The number of air intakes and their positioning generally results from the mission and is a function of the maximum incidences anticipated. Supersonic intake for missile has to provide adequate air mass flow with good pressure recovery at different flight regime at cruise as well as at the manoeuvring conditions, such as below and above the designed Mach number with different angles of attack and sideslip. Lauerell [10] studied experimentally the influence of the distance of the air intakes from the nose of the missile. Experimental investigations of Herrmann and Glhan [11] have brought out the difference of intake performance differed at different angles of attack (-30° <

Paper Code : V71 N3/1032-2019. Manuscript received on 23 Aug 2018. Reviewed, revised and accepted as a Full Length Contributed Paper on 21 May 2019

$\alpha < 30°$) when its axial position is varied along the missile body. Maintaining the steady operation of the intake at different flight conditions is also very challenging and adaptation of bleed system is suggested to mitigate the unstarting problem of the intake. Waserbauer et al. [12] and Ryu et al. [13] investigated the effect of a fixed geometry bleed on the intake performance. Heyes [14] presented important experimental studies for aerodynamic characteristics of a series of twin intake air-breathing missile configurations with flow through model. Various positions of twin intake configurations, different wing and tail configurations are investigated in detail. Positioning of two intakes at the windward side of the missile close to the combustion chamber was suggested to yield the ideal performance for a ramjet and provide better internal aerodynamics and less weight.

The flow field of ramjet powered aerospace vehicle is highly three dimensional and complex due to the asymmetric placement of air intakes and other protrusions and existing empirical engineering methodologies are inadequate for vehicle design. With the advent of powerful parallel computers, robust numerical schemes and improved physical modeling, Computational Fluid Dynamics (CFD) is playing an important role in overall vehicle design. Although, separate CFD simulations are carried out for intake [15, 16] and combustor [17, 18] for variable flow ducted rocket engines, an integrated CFD analysis comprising of external flow in vehicle fore-body and other external part and internal flow in the propulsion components are very much essential to address strong coupling of aerodynamics and propulsion in high speed ramjet vehicle and to have accurate estimate of overall aero-propulsive parameters. Integrated external and internal flow CFD analysis of high speed ramjet vehicle has not been referred adequately in the open literature. Saha et al. [19] simulated coupled external and internal flow field of installed air intakes of a solid fueled integral rocket ramjet at different angles of attack up to 6° and reported a good match of the computed performance parameters with experimental results. Murty et al. [20] generated aerodynamic characteristics of a liquid fuel ramjet technology demonstration vehicle through coupled external internal flow analysis and suggested design improvement. Bhandarkar et al. [21] simulated the flow through experimental model of twin intake, X-tail configuration of Heyes [14] to assess the predictive capabilities of commercial CFD tools and the computed aerodynamic and intake performances parameters matches well with the experimental results.

In the present work, non-reacting coupled external-internal flow simulations are carried out to estimate the effect of radome shape, intake bleed system and diverter height on the performance of a ducted ramjet missile. The missile operates in the Mach Number range 1.8 to 4 and the angle of attack varies from and -5° to 20°. The dimensions of the missile are constrained by the launch platform of the missile. The design Mach number and angle of attack is 2.3 and 0° respectively. Three dimensional Reynolds Averaged Navier Stokes (RANS) equations are solved along with SST-k ω turbulence model [22] using a commercial CFD package Ansys Fluent [23] software. Flow spillage and Intake performance for different Radom shapes, diverter heights and boundary layer diverters are compared.

The Configuration and Computational Details

As shown in Fig.1, the vehicle configuration consists of a radome, cylindrical body, rectangular twin air intake, boundary layer diverter, tapered fairing and X-tail fins. The computational domain considered for external-internal flow simulation is shown in Fig.2, which consists of conical external domain and flow through passage inside the body. The domain inlet starts at 2D ahead of the missile body and is extended up to 25 D, where D is missile diameter. The domain inlet and exit boundaries are kept 11 D (circular) and 42 D (circular) respectively. An unstructured grid of 2.7 million cells is generated using ICEM CFD [24]. Grids are very fine near nose, intake and wall regions to capture shocks and viscous affects accurately. The grid structure over a vertical plane and an intake plane is shown in Fig.3. The adequacy of the present grid is demonstrated through grid independence and grid convergence index studies presented later in the section.

Combined internal-external flow simulation is carried out by using commercial CFD software ANSYS Fluent 14.5 [23]. In the numerical simulation, compressible 3-D Navier Stokes equations are solved with SST k-ω turbulence model. A cell-centred finite volume method based on the linear reconstruction scheme that allows use of computational elements with arbitrary polyhedral topology, including quadrilateral, hexahedral, triangular, tetrahedral, pyramidal, prismatic and hybrid meshes is employed. Density based implicit coupled solver is chosen for solving the governing equations. Inviscid fluxes are discretized by 2^{nd} order accurate Roe scheme [25] whereas 2nd order central differencing scheme is used to discretize the viscous fluxes. Pressure, temperature and Mach number conditions are prescribed at the domain inflow and

supersonic outlet condition is prescribed at domain outlet. Reference area is missile cross section area, reference length is missile diameter, and reference flow conditions are taken from free stream with corresponding altitude and Mach number.

Grid Independence Study

Three different grid sizes 2.2, 2.7 and 5.4 million cells are generated for external airframe configuration to demonstrate the grid independence of the results. Overall drag coefficient for zero degree angle is estimated 0.442, 0.465, and 0.473 respectively for three different grids. Comparison of missile surface pressure along mid plane generator is plotted in Fig.4, which shows the close agreement between the three grids.

For steady state boundary-value problem, the main source of numerical error in CFD is iterative convergence or grid convergence error [26]. Grid convergence or discretization error, which is the error of the solution of the difference equations compared to the exact solution of the partial differential equation, is the major source of numerical error. This error can be estimated by running the solution in two different grids (coarse and fine). The simplest of such estimate is given by the relative difference [27], where f represent any quantity of interest and the indices 1 and 2 refer to the fine and coarse grid solution respectively. (In the present calculation, surface pressure has been taken as the parameter of interest) Roache [28] has proposed a Grid-Convergence Index (GCI) as an error based on uncertainty estimate of the numerical solution as

$$GCI = F_s \frac{1\,\varepsilon\,1}{(h_2/h_1)^p - 1}$$

where h is the order of grid spacing, p is the order of accuracy of numerical scheme and F_s is a factor of safety. Roache [29] has suggested $F_s = 3$ for minimal of two grid calculations. For the present calculation p is equal 2 with h_2 / h_1 equal to 2, GCI is order of ε. The axial distribution of the computed percentage error estimate based on pressure values between two grids are also presented in the Fig.5. Maximum error between two simulations is within 2%. This analysis indicates that the grid is adequate to capture most of features of the flow and the solution in grid independent.

Results and Discussion

Different numerical simulations are carried out to find out the effect of radome shape, boundary layer diverter height and the intake bleed system in the overall performance parameters of the intake and the results are compared.

Assessment of Radome Shape

The schematic of ogive and power law shaped radome is shown in Fig.5 and detailed CFD simulations were carried out at cruise condition for two different radome shapes for the estimation of aerodynamic drag coefficients and to assess the flow quality at the intake entry plane. It is seen that radome drag coefficient increases from 0.1 to 0.133 for the change in radome shape from ogive to power law. Overall drag coefficient increases by 0.081 (0.631-0.550) in power law as compared to ogive radome which accounts for almost 15% increase in external drag in the case of power law radome.

The velocity profile at the intake entry plane is plotted for the ogive and power law radome configurations in Fig.6. The velocity profile for the ogive radome is relatively cleaner and more uniform than that of the power law radome. The boundary layer thickness for the Ogive radome (3mm) is marginally lower than boundary layer thickness of power law radome (3.5 mm). The intake performance in terms of pressure recovery and mass capture ratio is compared for the two radome shapes in Table-1. The mass capture ratio and the total pressure recovery for the ogive radome is found marginally better than the power law radome shape.

Effect of Diverter Height

Simulations are carried out for design Mach number of 2.3 and zero degree angle of attack for two different heights of boundary layer diverter (0.05 D and 0.08 D) to find its effect on the intake performance. The axial veloc-

Table-1 : Intake Performance for Different Radome Shapes

Radome shape	Ogive radome	Power law radome	% difference
Mass capture ratio	0.95	0.94	1
Total pressure recovery	0.678	0.655	3.4

ity contour (shown in Fig.7) is clearly indicting that for higher diverter height (0.08D) the forebody boundary layer is not entering into intake. Intake performance parameters for the two boundary layer diverter heights are presented in Table-2 and a significant improvement in intake performance is observed for the higher boundary layer diverter height case.

Performance of Intake With and Without Bleed System

An intake is an important part of the air-breathing missile. It is designed to get a desired mass flow rate at combustor with a minimum pressure loss. Flow in the intake need to be steady and in started conditions. But the interaction of the incoming supersonic flow with the intake boundary layer can lead to significant adverse pressure gradient which may separate the flow. In case of flow separation, the shock system inside the intake cannot be contained within and the intake becomes unstarted [30]. For unstarted intake, there is significant increase in the spillage drag and decrease in the mass flow rate. To mitigate the unstarting problem and to avoid boundary-layer separation inside the intake, boundary-layer bleed and bypass systems are recommended [30]. The schematic of the bleed system adopted in the study is shown in Fig.8. Boundary-layer bleed systems is used to achieve operating stability, to avoid unstart of the intake, and to expand the missiles manoeuvring range. Inlet performance can be improved with modifications of the internal duct walls by varying the bleed slots and angle of bleed holes in relation to boundary-layer flow. The boundary layer bleed duct location is adjusted between the ramps and the subsonic diffuser depending on the boundary layer separation. Different simulations are carried out for the whole configuration with and without bleed system. The velocity contour near the intake with and without bleed system condition is shown in Fig.9. The significant spillage is observed near the intake forebody and the flow is seen separated from the centre body for the case without boundary layer bleed; whereas, no spillage and clean flow is seen in the intake for intake with bleed. The total pressure recovery with and without bleed is estimated at 0.745 and 0.678 respectively. An improvement of 9% is observed in the total pressure recovery due to boundary layer bleed system.

Table-2 : Intake Performance for Different Diverter Heights

Diverter height	0.08D	0.05D	% difference
Mass capture ratio	0.95	0.93	2.1
Total pressure recovery	0.678	0.60	11.5

Effect of Mach Number and Angle of Attack

Different combined external- internal flow simulations are carried out for different cruise Mach numbers and angles of attacks. Fig.10 presents the Mach number distributions at the intake plane for different Mach number and angle of attack combinations. For the same Mach number of 2.5 when angle of attack is increased from 0° to 10°, the oblique shock at the intake ramp moves upstream. A detached shock is formed in front of intake which diverts the incoming air, causing the spillage. As the Mach number is increased for the angle of attack of 10°, the shock moves closer to the intake cowl. It reduces the spillage and increases mass capture ratio. Computed pressure recovery and mass flow rates of the intake for different Mach numbers and angles of attack is shown in Tables-3 and Table-4 respectively. It is observed that the mass capture ratio decreases due to increase in spillage when the angle of attack increases for a particular Mach number of 2.5, while for a fixed angle of attack (AOA=10°) mass capture ratio increases with the increase of Mach number. As the free stream Mach number increases, the pressure recovery decreases due to shock losses. A shock appears in front of the intake entrance as the angle of attack increases, which increases losses, hence the pressure recovery reduces. Axial force coefficient (C_A), normal force coefficient

Table-3 : Intake Performance at Different Mach Numbers at 10° Angle of Attack

Sl. No.	Mach	AOA (deg)	Mass Capture Ratio	Pressure Recovery
1	2.5	10	0.78	0.65
2	3	10	0.97	0.6

Table-4 : Intake Performance at Different Angles of Attack at Cruise Mach Number

Sl. No.	Mach	AOA (deg)	Mass Capture Ratio	Pressure Recovery
1	2.5	0	0.95	0.68
2	2.5	10	0.78	0.65

Table-5 : Aerodynamic Parameters for Total (External + Internal) Configuration

Mach	AOA	C_A	C_N	C_m	X_{cp}/D
2.5	0	0.88	-0.27	--	--
2.5	10	1.02	3.9	48.01	12.32
3	10	0.88	3.98	49.36	12.40

(C_N), pitching moment coefficient (C_m) and centre pressure location from the nose tip are evaluated and listed in Table-5 for total configuration under various free stream flow conditions. The drastic change observed in the C_N and C_m for high angle of attack may be due to the asymmetric configuration of the missile.

Conclusions

Numerical simulation of a combined external-internal non-reacting flow path of a generic ducted flow ramjet configuration is performed. Three dimensional RANS equations are solved along with SST-Kω turbulence model. Grid independence of the results are demonstrated by not only comparing the results with different grids but also analyzing the Grid Convergence Index. Ogive radome provide comparatively lesser drag with improved intake performance compared to its power law counterpart. Increase of boundary layer height to 0.08D from 0.05D has improved the intake performance significantly. Inclusion of bleed system in the intake has reduced the spillage and improved the intake performance by 9%. It is observed that for same angle of attack, if Mach number increases, the mass capture is increased but pressure recovery detoriates; while, for fixed Mach number, increase in angle of attack reduces both mass capture and pressure recovery. The asymmetric configuration of the missile caused drastic change in the C_N and C_m for high angle of attack. It is demonstrated that use of high fidelity design tool is require to obtain improved aero-propulsive configuration of ducted ramjet missile. Coupled external-internal flow simulation with non-reacting simulation in the vehicle fore body, outer surface and reacting simulations in the ramjet engine is under progress to characterize complete aero-propulsive characterization of ducted ramjet missile.

References

1. Krishnan, S. and George, P., "Solid Fuel Ramjet Combustor Design", Progress in Aerospace Science, Vol.34, 1988, pp.219-256.

2. Waltrup, P. J., White, M. E., Zarlingo, F. and Gravlin, E. S., "History of U.S. Navy Ramjet, Scramjet, and Mixed-Cycle Propulsion Development", Journal of Propulsion and Power, Vol.18, No.1, January-February 2002, pp.14-27.

3. Fry, R. S., "A Century of Ramjet Propulsion Technology Evolution", Journal of Propulsion and Power, Vol.20, No.1, January-February 2004, pp.27-58.

4. Calzone, R. F., "Developments in Missile Ramjet Propulsion", Report No.TNO Report PML 1996-A100, 1996.

5. Besser, H. L. and Hermann, L. W., "The Ducted Rocket Propulsion System for Meteor and its Background in German Airbreathing Motor Technology", Paper No. ISABE-2005-1149.

6. Besser, H. L., Hermann. L. W. and Kurth, G., "Fit for Mission - Design Tailoring Aspects of throttleable Ducted Rocket Propulsion Systems", AIAA-2008-5262.

7. Moerel, J. L. P. A., Calzone, R. F., Halswijk, W. H. C., Horst, R. M. V., Stowed, R. and Lauzontt, M., "Performance Simulations of a Rocket and a Ramjet Air-to-Air Missile", AIAA-2001-4412.

8. Besser, H. L., "History of Ducted Rocket Development at Bayern-Chemie", AIAA-2008-5261.

9. Yoshihiro, Y., Yoshiyuki, I., Hisahiro, N., Eishu, K., Junichi, S., Yuichi, O. and Akihiko, Y., "Performance Demonstration of a Variable Flow Ducted Rocket Engine by Test Flight", AIAA-2009-5031.

10. Laruelle, G., "Air Intakes for a Probative Missile of Rocket Ramjet", NASA TM-77407, 1984.

11. Herrmann, D. and Gülhan, A., "Influence of Intake Orientation on Ramjet Performance", Journal of Propulsion and Power, Vol.26, No.4, July-August 2010, pp.848-857.

12. Wasserbauer, J., Shaw, R. and Neumann, H., "Minimizing Boundary Layer Bleed for a Mixed Compression Inlet", AIAA Paper No.1973-1270, 1973.

13. Ryu, K. J., Lim, S. and Song, D. J., "A Computational Study of the Effect of Angles of Attack on a Double-

cone Type Supersonic Inlet with a Bleeding System", Computers and Fluids, Vol.50, 2011, pp.72-80.

14. Hayes, C., "Aerodynamic Characteristics of a Series of Twin-Inlet Airbreathing Missile Configurations", NASA Technical Memorandum 84559, Langley Research Center, Virginia, 1983.

15. Moerel, J. L., Veraar, R. G., Halswijk, W. H. C., Pimentel, R., Corriveau, D., Hamel, N., Lesage, F. and Vos, J. B., "Internal Flow Characteristics of a Rectangular Ramjet Air Intake", AIAA Paper 2009-5076.

16. Hidenori, T., Kenji, K., Yoshiyuki, I., Junichi, S. and Akihiko, Y., "Development of Wide-range Supersonic Intake for Variable Flow Ducted Rocket Engine", AIAA Paper 2009-5223.

17. Stowe, R. A., Champlain, A. D. and Mayer, A. E. H. J., "Modelling Combustor Performance of a Ducted Rocket", AIAA Paper 2000-3728.

18. Ristori, A. and Dufour, E., "Numerical Simulation of Ducted Rocket Motor", AIAA Paper 2001-3193.

19. Saha, S., Sinha, P. K. and Chakraborty, D., "CFD Prediction of Ramjet Intake Characteristics at Angle of Attack", Journal of Aerospace Sciences and Technologies, Vol.62, No.3, 2010, pp.159-165.

20. Chandra Murty, M. S. R. and Chakraborty, D., "Coupled external and internal flow simulation of a Liquid Fuelled Ramjet Vehicle", Journal of Aerospace Science and Technology, Vol.36, 2014, pp.1-4.

21. Anand Bhandarkar., Souraseni Basu., Manna, P. and Chakraborty, D., "Aerodynamic Characterization of Ramjet Missile Through Combined External-Internal CFD Simulation", Defense Science Journal, Vol.66, No.6, November, 2016.

22. Menter, F. R., "Two-Equation Eddy-Viscosity Turbulence Models for Engineering Applications", AIAA Journal, Vol.32, No.8, 1994, pp.1598-1605.

23. Ansys Fluent 14.5 Theory and Users Guide, India, AnsysInc, 2013.

24. ICEM CFD 14.5 Modeling and Meshing Guide, India, AnsysInc, 2013.

25. Roe, P. L., "Characteristic Based Schemes for the Euler Equations", Annual Review of Fluid Mechanics, 18:337-365, 1986.

26. Guide for the Verification and Validation of Computational Fluid Dynamic Simulation G-077-1998, AIAA, Reston, VA, 1998.

27. Cutler, A.D., Danehy, P. M., O'Byrne, S., Rodrigues, C. G. and Drummond, J. P., "Supersonic Combustion Experiment for CFD Model Development and Validation", AIAA Paper No. 2004-266.

28. Roache, P. J., "Error base for CFD", AIAA Paper No. 2003-0408.

29. Roache, P. J., "Verification and Validation in Computational Science and Engineering", Hermon Publishers, New Mexico, 1998.

30. Seddon, J. and Goldsmith, E., "Intake Aerodynamics", Second Edition. Washington, DC: American Institute of Aeronautics and Astronautics, Inc, 1999.

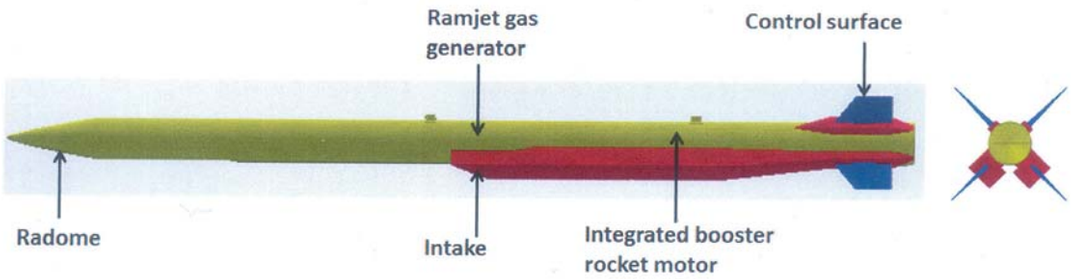

Fig.1 Schematic of Variable Flow Ducted Rocket Engine

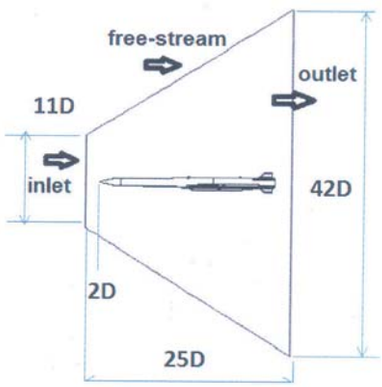

Fig.2 Computational Domain

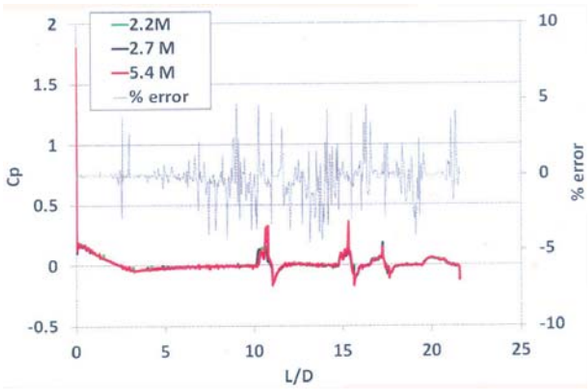

Fig.4 Comparison of Wall Pressure Along Mid Plane Generator for Three Different Grids

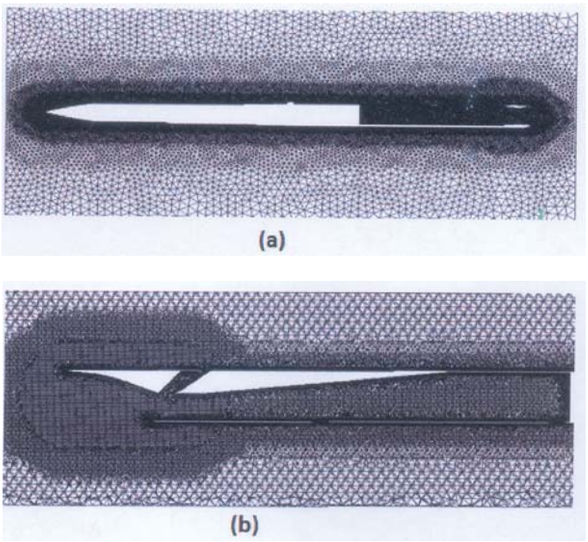

Fig.3 Grid Structure in (a) Vertical Plane (b) Intake Plane

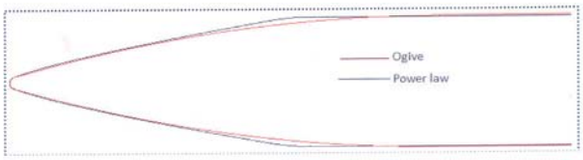

Fig.5 Comparison Between (a) Ogive and (b) Power Law Radome Shape

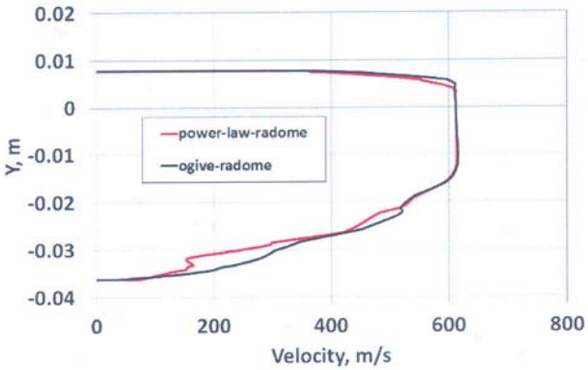

Fig.6 Velocity Profile at the Intake Plane of the Missile

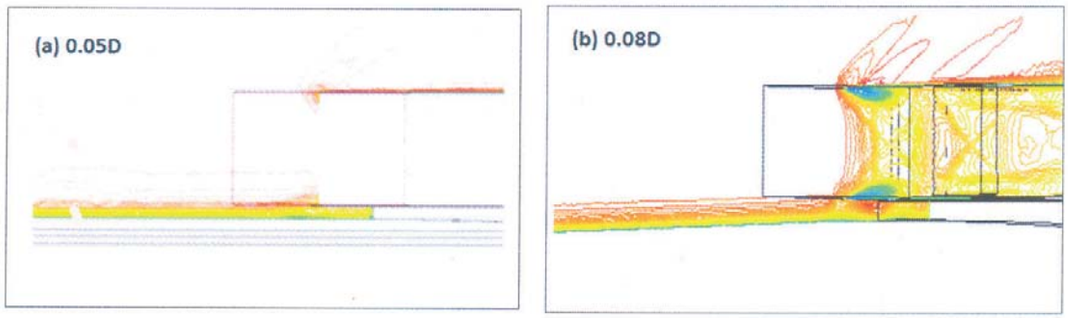

Fig.7 Boundary Layer Growth Near Air-intake for Diverter Heights (a) 0.05D (b) 0.08D

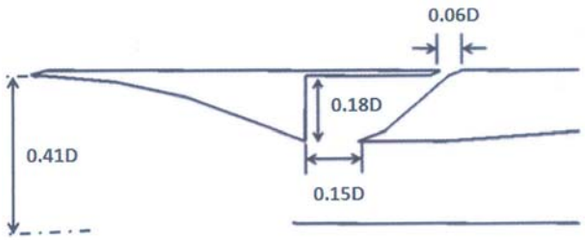

Fig.8 Boundary Layer Bleed System

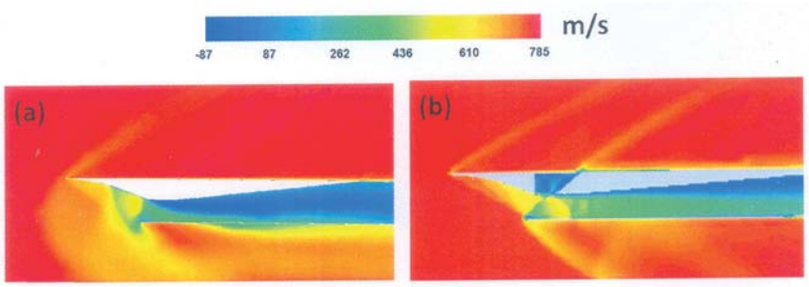

Fig.9 Velocity Contour at Intake Plane (M=2.4, AOA=0°) (a) Without Bleed (b) With Bleed

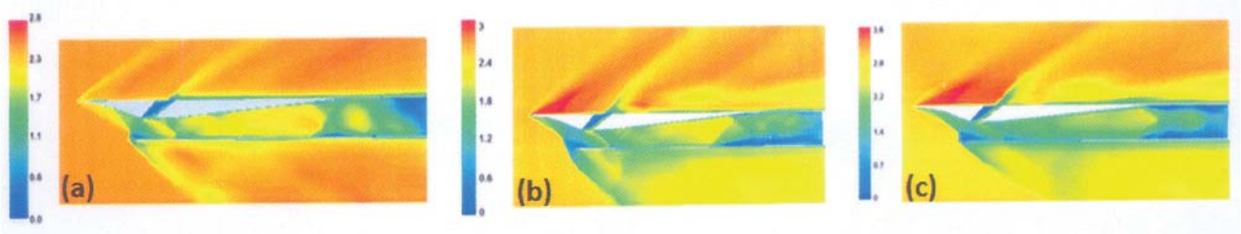

Fig.10 Mach Contour in Intake Plane (a) M=2.5, α=0° (b) 2.5, α=10° (c) M=3, α=10°